

Spin-Orbit-Driven Coherent Oscillations in a Few-Electron Quantum Dot

Stefan DeBald

Institut für Theoretische Physik, Universität Hamburg, Jungiusstrasse 9, 20355 Hamburg, Germany

Clive Emary

Instituut-Lorentz, Universiteit Leiden, P.O. Box 9506, 2300 RA Leiden, The Netherlands

(Received 28 October 2004; published 8 June 2005)

We propose an experiment to observe coherent oscillations in a single quantum dot with the oscillations driven by spin-orbit interaction. This is achieved without spin-polarized leads, and relies on changing the strength of the spin-orbit coupling via an applied gate pulse. We derive an effective model of this system which is formally equivalent to the Jaynes-Cummings model of quantum optics. For parameters relevant to an InGaAs dot, we calculate a Rabi frequency of 2 GHz.

DOI: 10.1103/PhysRevLett.94.226803

PACS numbers: 73.63.Kv, 03.65.-w, 71.70.Ej

Motivated by the desire for a closer understanding of quantum coherence and by the drive to develop novel quantum computing architecture, a number of breakthrough solid-state experiments have focused on coherent oscillations—the back and forth flopping of that most fundamental of quantum objects, the two-level system [1–4]. The pioneering work of Nakamura *et al.* with the coherent superposition of charge states of a Cooper-pair box [1] first demonstrated the possibility of observing such oscillations in a wholly solid-state device, thus sparking the remarkable progress in qubit development in superconducting systems [2,3].

The important double quantum dot experiment of Hayashi and co-workers [4] showed that coherent oscillations could also be observed in normal semiconductor systems. It is the purpose of this Letter to propose an experiment in which coherent oscillations are observed in a *single quantum dot* (QD), with these oscillations being driven by the spin-orbit (SO) interaction.

The SO interaction in semiconductor heterostructures has its origin in the breaking of inversion symmetry, and is increasingly coming to be seen as a tool with which to manipulate electronic states; see, e.g., [5]. The grandfather of these ideas is the spin transistor of Datta and Das [6], in which the SO interaction causes electron spins to precess as they move through a two-dimensional electron gas (2DEG). In materials where the structural inversion asymmetry dominates, e.g., InGaAs, the SO interaction can be described by the Rashba Hamiltonian [7]

$$H_{\text{SO}} = -\frac{\alpha}{\hbar} \left[(\mathbf{p} + \frac{e}{c} \mathbf{A}) \times \boldsymbol{\sigma} \right]_z. \quad (1)$$

In this Letter we consider the effects of H_{SO} on electrons in a small, few-electron lateral quantum dot. Although such dots are yet to be realized in materials with strong SO coupling, there is currently a considerable effort to develop nanostructures in such materials [8]. Our interest here is not in open or chaotic QDs [9,10], but rather in small dots in the Coulomb blockade regime.

Such dots have been studied by a number of authors [11–13], but our analysis differs in a crucial respect: by making an analogy with quantum optics, we are able to derive an approximate Hamiltonian that captures the essential physics of the dot. This model is formally identical to the Jaynes-Cummings (JC) model [14], first derived in the context of the atom-light interaction. Here, the roles of the atomic pseudospin and light field are played by the spin and orbital angular momentum of the electron, respectively. The system then naturally decomposes into a set of two-level systems (TLS), any of which may be considered as the qubit degree of freedom within which coherent oscillations can occur. These oscillations are genuine Rabi oscillations [15], with orbital and spin degrees of freedom exchanging excitation. This “spin-orbit pendulum” behavior has been noted in three-dimensional models in nuclear physics [16].

Having elucidated the origin and properties of the TLS, we then describe an experimental scheme through which the coherent oscillations can be investigated. The key problem here is that of injecting into, and reading out from, states which are not eigenstates of the SO coupled system. In the Hayashi experiment [4], this was achieved through the spatial separation of the two dots, which makes the leads couple to the localized left and right states, rather than to the bonding and antibonding eigenstates. In our single dot system, the direct analogy of this would be the injection of spin-polarized electrons. Given the difficulty of interfacing ferromagnetic leads with semiconductors [8], we avoid their use by exploiting the fact that the strength of the SO interaction can be controlled by external gates [17–19].

Our starting point is the Fock-Darwin theory of a single electron in a 2DEG with parabolic confinement of energy $\hbar\omega_0$ [20],

$$H_0 = \frac{(\mathbf{p} + \frac{e}{c} \mathbf{A})^2}{2m} + \frac{m}{2} \omega_0^2 (x^2 + y^2), \quad (2)$$

where m is the effective mass of the electron. Applying a

perpendicular magnetic field in the symmetric gauge, in second quantized notation we have

$$H_0 = \hbar\tilde{\omega}(a_x^\dagger a_x + a_y^\dagger a_y + 1) + \frac{\hbar\omega_c}{2i}(a_y a_x^\dagger - a_x a_y^\dagger), \quad (3)$$

with $\omega_c \equiv eB/mc$ and $\tilde{\omega}^2 \equiv \omega_0^2 + \omega_c^2/4$. The introduction of $a_\pm \equiv 2^{-1/2}(a_x \mp ia_y)$ decouples the system into eigenmodes of frequency $\omega_\pm = \tilde{\omega} \pm \omega_c/2$.

We now include the Rashba interaction of Eq. (1), for which the coupling strength α is related to the spin precession length $l_{SO} \equiv \hbar^2/2m\alpha$. With magnetic length $l_B \equiv \sqrt{\hbar/m\omega_c}$, we have

$$H_{SO} = \frac{\alpha}{\tilde{l}}[\gamma_+(a_+\sigma_+ + a_+^\dagger\sigma_-) - \gamma_-(a_-\sigma_- + a_-^\dagger\sigma_+)], \quad (4)$$

with coefficients $\gamma_\pm \equiv 1 \pm \frac{1}{2}(\tilde{l}/l_B)^2$ and $\tilde{l} \equiv \sqrt{\hbar/m\tilde{\omega}}$.

Adding the Zeeman term, in which we take g to be negative as in InGaAs, performing a unitary rotation of the spin such that $\sigma_z \rightarrow -\sigma_z$ and $\sigma_\pm \rightarrow -\sigma_\mp$, and rescaling energies by $\hbar\omega_0$, we arrive at the Hamiltonian

$$H = \omega_+ a_+^\dagger a_+ + \omega_- a_-^\dagger a_- + \frac{1}{2}E_z \sigma_z + \frac{l_0^2}{2\tilde{l}l_{SO}} \times [\gamma_-(a_-\sigma_+ + a_-^\dagger\sigma_-) - \gamma_+(a_+\sigma_- + a_+^\dagger\sigma_+)], \quad (5)$$

where $l_0 = \sqrt{\hbar/m\omega_0}$ is the confinement length of the dot and $E_z = |g|m/(2m_e)(l_B/l_0)^2$ is the Zeeman energy with m_e the bare mass of the electron.

This single-particle picture is motivated by the good agreement between Fock-Darwin theory and experiment in the non-SO case [20], and by studies which have shown that many-body effects in QDs play only a small role at the magnetic fields we consider here [11,12,21].

We now derive an approximate form of this Hamiltonian by borrowing the observation from quantum optics that the terms preceded by γ_+ in Eq. (5) are counterrotating, and thus negligible under the rotating-wave approximation [15] when the SO coupling is small compared to the confinement. This decouples the ω_+ mode from the rest of the system, giving $H = \omega_+ n_+ + H_{JC}$ where

$$H_{JC}(\alpha) = \omega_- a_-^\dagger a_- + \frac{1}{2}E_z \sigma_z + \lambda(a_-\sigma_+ + a_-^\dagger\sigma_-), \quad (6)$$

with $\lambda = l_0^2\gamma_-/2\tilde{l}l_{SO}$. This is the well-known Jaynes-Cummings model (JCM) of quantum optics. It is completely integrable, and has ground state $|0, \downarrow\rangle$ with energy $E_G = -E_z/2$ independent of coupling. The rest of the JCM Hilbert space decomposes into two-dimensional subspaces $\{|n, \uparrow\rangle, |n+1, \downarrow\rangle; n = 0, 1, \dots\}$. Diagonalization in each subspace gives the energies $E_\alpha^{(n,\pm)} = (n+1/2)\omega_- \pm \Delta_n/2$ with detuning $\delta \equiv \omega_- - E_z$ and $\Delta_n \equiv \sqrt{\delta^2 + 4\lambda^2(n+1)}$. The eigenstates are

$$|\psi_\alpha^{(n,\pm)}\rangle = \cos\theta_\alpha^{(n,\pm)}|n, \uparrow\rangle + \sin\theta_\alpha^{(n,\pm)}|n+1, \downarrow\rangle, \quad (7)$$

with $\tan\theta_\alpha^{(n,\pm)} = (\delta \pm \Delta_n)/2\lambda\sqrt{(n+1)}$.

Figure 1(a) shows a portion of the excitation spectrum obtained by exact numerical diagonalization for a typical dot in InGaAs. The approximate H_{JC} describes the energy levels of the system to within 10% of the typical anticrossing width and 1% of ω_0 . This small discrepancy is visible in Fig. 1(b). In the following, we are concerned only with the lowest-lying energy states in the dots. Without SO interaction, these states are described by $n_+ = 0$, indicating that the states converge to the lowest Landau level in the high-field limit, and by n_- corresponding to the quantum number of angular momentum. The SO interaction thus couples two states of adjacent angular momentum and opposite spin. The detuning δ uniquely identifies ω_c for fixed material parameters and dot size.

Under the assumptions of the constant interaction model [20], the most important prediction of this model for linear transport is that, with the dot on resonance, the addition-energy spectrum for the first few electrons (up to 18 here) is described by a sequence of well separated anticrossings, the width of which increases as $\alpha\sqrt{n+1}$. This behavior is shown in Fig. 1(c), and its observation would be confirmation of our JC model, and would permit a determination of α in quantum dots.

We now describe the procedure for observing spin-orbit-driven Rabi oscillations. Our proposal is somewhat similar to that of Nakamura [1] with a voltage pulse driving the system, but with the crucial difference that the oscillations here are induced not by a change in the detuning, but by a change in the SO coupling strength. We operate in the

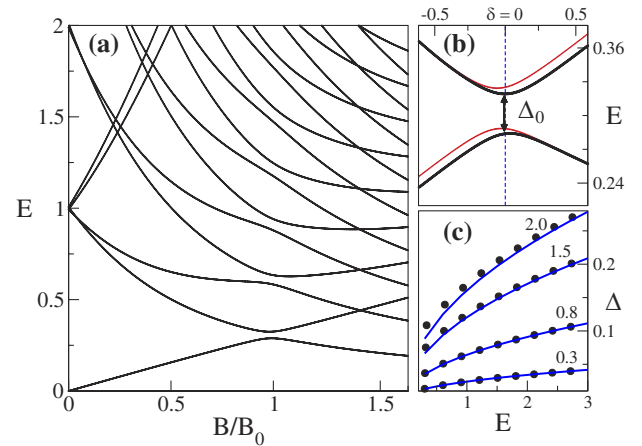


FIG. 1 (color online). Spectral features of the Rashba-coupled quantum dot as a function of magnetic field. The parameters used are typical of InGaAs: $g = -4$, $m/m_e = 0.05$ with dot size $l_0 = 150$ nm. Resonance occurs at $B_0 = 90$ mT. (a) Low-lying excitation spectrum for spin-orbit coupling $\alpha = 0.8 \times 10^{-12}$ eV m. (b) Lowest-lying anticrossing. The thick line is the JC model showing anticrossing width Δ_0 at $\delta = 0$, and the thin line is the exact numerical result. (c) Plot of width Δ_n against central energy of anticrossing with the dot on resonance for different α in the range $(0.3-2.0) \times 10^{-12}$ eV m. The exact numerical results (circles) show excellent agreement with the square-root behavior predicted by the JC model in this α range.

nonlinear transport regime and address a single two-level system by being near resonance and by tuning the chemical potentials of the leads close to the n th anticrossing. The SO coupling is set to α_1 and the states taking part in the oscillation are eigenstates of $H_{JC}(\alpha_1)$, namely $\psi_{\alpha_1}^{\pm}$, which are situated symmetrically around the chemical potential of the right lead μ_R ; see Fig. 2(a). The temperature is taken smaller than the detuning $k_B T \ll \delta$ to avoid the effects of thermal broadening. Assuming Coulomb blockade and considering first-order sequential tunneling only, electrons can either tunnel from the left lead into the dot via state $\psi_{\alpha_1}^+$ and subsequently leave to the right or, alternatively, tunnel to state $\psi_{\alpha_1}^-$ blocking the dot; see Fig. 2(b). Assuming tunneling through the left or right barrier at a constant rate $\Gamma_{L/R}$, we set $\Gamma_L > \Gamma_R$ to assure that the dot is preferentially filled from the left, thus maximizing the current. On average then, the dot is initialized in state $\psi_{\alpha_1}^-$ for times $t_i > \Gamma_R^{-1}$.

Having trapped an electron in this state, we apply a voltage pulse to the gate. This has two effects. First, this change in voltage alters the SO coupling to a new value α_2 . Since this change is performed nonadiabatically, the electron remains in the initial eigenstate $\psi_{\alpha_1}^-$ until Rabi oscillations begin between this state and $\psi_{\alpha_1}^+$ under the influence of the new Hamiltonian $H_{JC}(\alpha_2)$. Second, the TLS is drawn

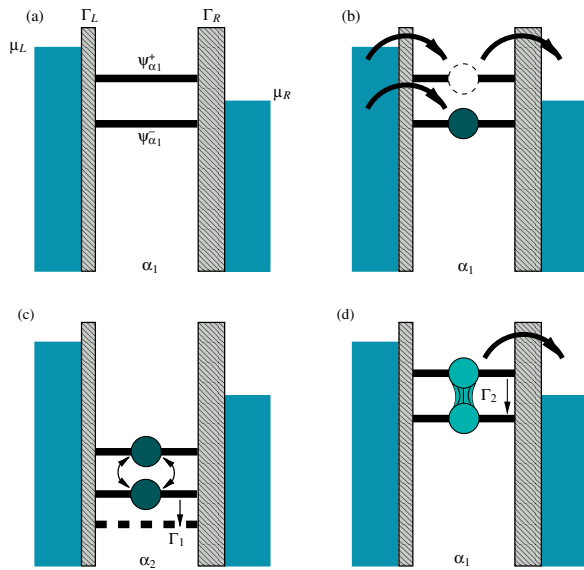


FIG. 2 (color online). Configuration of the dot in the various stages of the cycle. (a) The positions of the dot levels $\psi_{\alpha_1}^{\pm}$, chemical potentials $\mu_{L,R}$, and the tunneling rates $\Gamma_L > \Gamma_R$. (b) The coupling is initially α_1 . On average, for times $t_i > \Gamma_R^{-1}$ the dot will be initialized in state $\psi_{\alpha_1}^-$. (c) The applied voltage pulse lowers the dot levels and nonadiabatically changes the coupling to $\alpha_2 \neq \alpha_1$, thus inducing Rabi oscillations. (d) Pulse is switched off after time t_p and the levels return to their initial places. Tunneling to the right occurs when the electron has oscillated into the upper state. Relaxation rates $\Gamma_{1,2}$ are also shown.

below both chemical potentials, assuring that oscillations can occur without tunneling out of the dot; see Fig. 2(c).

After a time t_p , the gate voltage is returned to its initial value, and the TLS resumes both its original position and coupling α_1 , as in Fig. 2(d). Tunneling out of the dot can now occur, provided that the electron is found in the upper state, which happens with a probability given by the overlap of the oscillating wave function at time t_p with the upper level,

$$P(t_p) = |\langle \psi_{\alpha_1}^+ | \Psi(t_p) \rangle|^2 = |\langle \psi_{\alpha_1}^+ | e^{-iH(\alpha_2)t_p} | \psi_{\alpha_1}^- \rangle|^2. \quad (8)$$

This process is operated as a cycle and the current is measured. From probability arguments we see that $I \approx e\Gamma_R P(t_p)$, where we have used the simplification that $\Gamma_R^{-1} > t_p, \Gamma_L^{-1}$. Thus, by sweeping t_p we are able to image the time evolution of Rabi oscillations, just as in the previous experiments of Nakamura and Hayashi.

The singular case of a nonadiabatic change in α from zero to a finite value produces oscillations with the maximum possible amplitude, $P_{\max} = 1$. However, in realistic systems only changes between finite values of α are feasible. This leads to a reduction in the amplitude, and achieving a significant oscillation signal requires a suitably large change in α . In experiments with 2DEGs, changes in α of a factor of 2 are reported, and in a recent Letter by Koga *et al.*, α was shown to vary in the range $\approx (0.3-1.5) \times 10^{-12}$ eV m (a factor of 5) in one InGaAs sample [19]. Grundler [18] has shown that the large back-gate voltages usually used to change α can be drastically reduced by placing the gates closer to the 2DEG. Thus, it is conceivable that changes in α of a factor

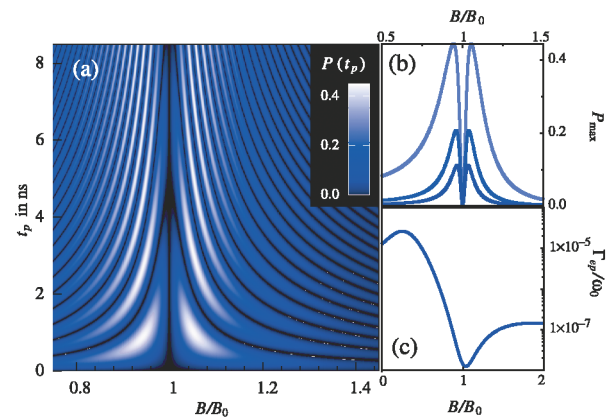


FIG. 3 (color). Characteristics of the Rabi oscillation. (a) Probability $P(t_p)$ of finding an electron in the upper level after time t_p following the nonadiabatic change $\alpha_1 = 1.5 \rightarrow \alpha_2 = 0.3 \times 10^{-12}$ eV m as a function of magnetic field. (b) Amplitude of oscillation as a function of B/B_0 for changing from $\alpha_1 = 1.5, 0.8, 0.6$ to $\alpha_2 = 0.3 \times 10^{-12}$ eV m (top to bottom). (c) Phonon-induced relaxation rate for InAs parameters $\alpha = 1.5 \times 10^{-12}$ eV m, $P = 3.0 \times 10^{-21}$ J²/m², $\rho = 5.7 \times 10^3$ kg/m³, $c = 3.8 \times 10^3$ m/s. Close to B_0 the rate is suppressed to $\Gamma_{ep} < 10^{-7} \omega_0$.

between 2 and 5 could be produced with voltages small enough to be pulsed with rise times substantially shorter than a typical coherent oscillation period.

In Fig. 3(a) we plot time traces of the transition probability $P(t_p)$ calculated for the first anticrossing as a function of magnetic field. We have used the values $\alpha_1 = 1.5 \times 10^{-12}$ eVm and $\alpha_2 = 0.3 \times 10^{-12}$ eVm from the Koga experiment [19]. The amplitude of the oscillations P_{\max} for different ratios of α_2/α_1 is presented in Fig. 3(b), which shows a node at $B = B_0$ ($\delta = 0$). This is because, for $\delta = 0$, the eigenstates of JCM are $2^{-1/2}(|n, \uparrow\rangle \pm |n+1, \downarrow\rangle)$ for all $\alpha \neq 0$. Therefore, a finite detuning is required to obtain the maximum amplitude, which concurs with $\delta > k_B T, \Gamma_R$ to overcome broadening effects. Both the amplitude P_{\max} and frequency Ω show nontrivial dependencies on α_1 and α_2 as well as on the magnetic field. This latter behavior stems from the parametric dependence on B of all three parameters in H_{JC} .

For our model parameters with $\alpha_2/\alpha_1 = 1/5$ and with the detuning set such that the amplitude is maximized, we have $P_{\max} \approx 0.45$ with a Rabi frequency of $\Omega = 2$ GHz, which corresponds to a period of about 3 ns. This is within accessible range of state-of-the-art experimental technique. Note that the period can be extended by using weaker confinement and SO coupling.

For both the observation of coherent oscillations and the operation as a qubit, it is essential that the lifetime of state ψ_α^+ is long. This is the case for a pure electronic spin in a QD [8,22], and we now show that the hybridization of the spin with the orbitals, and the ensuing interaction phonons, does not affect this. We assume a piezoelectric coupling to acoustic phonons via the potential $V_{ep} = \lambda_{\mathbf{q}} e^{i\mathbf{q}\cdot\mathbf{r}} (b_{\mathbf{q}} + b_{-\mathbf{q}}^\dagger)$, with phonon operators $b_{\mathbf{q}}$ and $|\lambda_{\mathbf{q}}|^2 = \hbar P / 2\rho c q \mathcal{V}$, with coupling P , mass density ρ , speed of sound c , and volume \mathcal{V} [23]. For $n = 0$, a golden rule calculation yields the rate

$$\Gamma_{ep}/\omega_0 = \frac{mP}{8\pi(\hbar\omega_s)^2\rho l_0} \frac{\sqrt{2}l_0}{\tilde{l}} \sin^2\theta_+ \sin^2\theta_- \xi^5 I(\xi), \quad (9)$$

with $\omega_s = c/l_0$, $\xi = 2^{-1/2}(\tilde{l}/l_0)(\Delta/\hbar\omega_s)$, and $I(\xi) \leq 8/15$. Close to B_0 , $\xi \ll 1$, and thus the rate is extremely small $\Gamma_{ep} \approx 10^4 \text{ s}^{-1}$ [Fig. 3(c)]. Therefore, the robustness of spin qubits is not significantly weakened by the SO hybridization.

In general, residual relaxation affects our measurement scheme in two ways. During the oscillation [Fig. 2(c)], the system may relax to the eigenstate $\psi_{\alpha_2}^-$. This damps the oscillation by a factor $\exp(-\Gamma_1 t_p)$ to the constant value $I = e\Gamma_R P_{\max}/2$. Relaxation during the readout phase [Fig. 2(d)] simply reduces the overall amplitude of the signal by a factor $\exp(-\Gamma_2/\Gamma_R)$. Clearly then, to observe oscillations, we require $\Gamma_1 < \Omega$ and $\Gamma_2 < \Gamma_R$.

In summary, we have outlined a proposal for the observation of spin-orbit-driven coherent oscillations in a single quantum dot. We have derived an approximate model,

inspired by quantum optics, that shows the oscillating degree of freedom to represent a novel, composite spin-angular momentum qubit.

This work was supported by the EU via TMR/RTN projects, and the German and Dutch Science Foundations DFG, NWO/FOM. We are grateful to T. Brandes, C. W. J. Beenakker, and D. Grundler for discussions, and to B. Kramer for guidance and hospitality in Hamburg.

-
- [1] Y. Nakamura, Yu. A. Pashkin, and J. S. Tsai, *Nature* (London) **398**, 786 (1999).
 - [2] D. Vion *et al.*, *Science* **296**, 886 (2002).
 - [3] I. Chiorescu, Y. Nakamura, C. J. P. M. Harmans, and J. E. Mooij, *Science* **299**, 1869 (2003).
 - [4] T. Hayashi *et al.*, *Phys. Rev. Lett.* **91**, 226804 (2003).
 - [5] J. C. Egues, G. Burkard, and D. Loss, *Phys. Rev. Lett.* **89**, 176401 (2002); E. I. Rashba and A. L. Efros, *Phys. Rev. Lett.* **91**, 126405 (2003).
 - [6] S. Datta and B. Das, *Appl. Phys. Lett.* **56**, 665 (1990).
 - [7] Yu. A. Buchkov and E. I. Rashba, *JETP Lett.* **39**, 78 (1984); *J. Phys. C* **17**, 6039 (1984).
 - [8] I. Žutić, J. Fabian, and S. Das Sarma, *Rev. Mod. Phys.* **76**, 323 (2004), and references therein.
 - [9] J. A. Folk *et al.*, *Phys. Rev. Lett.* **86**, 2102 (2001); B. I. Halperin *et al.*, *ibid.* **86**, 2106 (2001); I. L. Aleiner and V. I. Fal'ko, *ibid.* **87**, 256801 (2001).
 - [10] J. H. Creemers, P. W. Brouwer, and V. I. Fal'ko, *Phys. Rev. B* **68**, 125329 (2003).
 - [11] J. Könemann, R. J. Haug, D. K. Maude, V. I. Fal'ko, and B. L. Altshuler, *cond-mat/0409054*.
 - [12] T. Chakraborty and P. Pietiläinen, *cond-mat/0410248*.
 - [13] R. de Sousa and S. Das Sarma, *Phys. Rev. B* **68**, 155330 (2003); O. Voskoboynikov, O. Bauga, C. P. Lee, and O. Tretyak, *J. Appl. Phys.* **94**, 5891 (2003); M. Governale, *Phys. Rev. Lett.* **89**, 206802 (2002); M. Valín-Rodríguez, A. Puente, L. Serra, and E. Lipparini, *Phys. Rev. B* **66**, 235322 (2002); O. Voskoboynikov, C. P. Lee, and O. Tretyak, *ibid.* **63**, 165306 (2001).
 - [14] E. T. Jaynes and F. W. Cummings, *Proc. IEEE* **51**, 89 (1963).
 - [15] L. Allen and J. H. Eberly, *Optical Resonance and Two-level Atoms* (Wiley, New York, 1975).
 - [16] R. Arvieu and P. Rozmej, *Phys. Rev. A* **50**, 4376 (1994); **51**, 104 (1995).
 - [17] J. Nitta, T. Akazaki, H. Takayanagi, and T. Enoki, *Phys. Rev. Lett.* **78**, 1335 (1997).
 - [18] D. Grundler, *Phys. Rev. Lett.* **84**, 6074 (2000).
 - [19] T. Koga, J. Nitta, T. Akazaki, and H. Takayanagi, *Phys. Rev. Lett.* **89**, 046801 (2002).
 - [20] L. P. Kouwenhoven, D. G. Austing, and S. Tarucha, *Rep. Prog. Phys.* **64**, 701 (2001).
 - [21] U. Merkt, J. Huser, and M. Wagner, *Phys. Rev. B* **43**, 7320 (1991).
 - [22] A. V. Khaetskii and Y. V. Nazarov, *Phys. Rev. B* **61**, 12 639 (2000).
 - [23] M. Bruus, K. Flensberg, and H. Smith, *Phys. Rev. B* **48**, 11 144 (1993).